

Estimation of Erosion Rate by Absorption Spectroscopy in a Hall Thruster

IEPC-2005-037

Presented at the 29th International Electric Propulsion Conference, Princeton University,
October 31 – November 4, 2005

Naoji Yamamoto *

Graduate School of Engineering Sciences, Kyushu University, Kasuga, Fukuoka 816-8580, Japan

Shigeru Yokota,[†] Makoto Matsui,[‡] Kimiya Komurasaki,[§] and Yoshihiro Arakawa^{**}
The University of Tokyo, City, Bunkyo-ku, Tokyo, 113-8656, Japan

Abstract: The erosion rate of a Hall thruster was estimated with the objective of building a real-time erosion rate monitoring system using a 1 kW class anode layer type Hall thruster. This system aids the understanding of the trade-off between lifetime and performance. To estimate the flux of the sputtered wall material, the number density of the sputtered iron was measured by laser absorption spectroscopy using an absorption line from ground atomic iron at 371.9935 nm. An ultraviolet $\text{Al}_x\text{In}_y\text{Ga}_{(1-x-y)}\text{N}$ diode laser was used as the probe. The estimated number density of iron was $1.1 \times 10^{16} \text{ m}^{-3}$, which is reasonable when compared with that measured by duration erosion tests. The relation between estimated erosion rate and magnetic flux density also agreed with that measured by duration erosion tests.

I. Introduction

Hall thrusters show considerable promise for satellite station keeping and orbit transfer applications^{1,2} since they offer an attractive combination of high thrust efficiency, exceeding 50%, with a specific impulse range of 1,000-3,000 s and a higher ion beam density than ion thrusters. This is because Hall thrusters are not space-charge limited.³

Several types of Hall thrusters are available, but they can be categorized into two general groups; the anode layer type and the magnetic layer type.^{4,5} One of the former type is the “Thruster with Anode Layer” (TAL), which has been developed in Russia.^{6,7} This thruster has a narrow acceleration zone for reducing the loss of ions and electrons due to collisions with the walls.^{8,9} It has a conducting wall maintained at the cathode potential, and its acceleration channel length is shorter than its channel width.¹⁰ The electron temperature of this type is higher than that of the other because of the no electron energy losses to the cathode potential wall.⁵ The wall, or guard ring, protects the magnetic poles from ion bombardment. It is made of highly resistive materials against sputtering ions, such as pyrolytic graphite or stainless steel.¹¹ The short acceleration length and the highly resistive material will give the thruster the potential to have a longer lifetime than that which has been displayed by SPT's.⁹

Lifetime is one of the most significant performance criteria for electric propulsion systems. There have been many studies on the lifetime of Hall thrusters, including endurance tests,^{12,13} and erosion measurements.^{10,14} These studies show that the erosion of the acceleration channel wall is the main factor limiting the lifetime of Hall thruster and that the erosion depends on operating condition, magnetic field configuration, wall material, anode

* Research Associate, Department of Advanced Energy Engineering Science, yamamoto@aees.kyushu-u.ac.jp

† Graduate student, Department of Aeronautics and Astronautics, yokota@al.t.u-tokyo.ac.jp.

‡ Research Fellow, Department of Aeronautics and Astronautics, matsui@al.t.u-tokyo.ac.jp.

§ Associate Professor, Department of Aeronautics and Astronautics, komurasaki@k.u-tokyo.ac.jp

** Professor, Department of Aeronautics and Astronautics, arakawa@al.t.u-tokyo.ac.jp

configuration, and channel geometry. Understanding this dependence is essential for the practical application of Hall thrusters. It is not, however, practicable to validate the lifetime at each condition by means of typical wear tests because of the huge costs in time and money. Therefore, the measurement of the erosion rate by Laser Absorption Spectroscopy^{15, 16} is proposed. LAS has many advantages: 1) it could provide real-time monitoring of the erosion rate, 2) it is a non-intrusive optical method for measuring the properties of plasmas, 3) it does not require absolute calibration, though a calibrated light source or a density reference cell is used in Laser Induced Fluorescence or emission spectroscopy,^{17, 18} since number density of the absorbing atom can be deduced from the absorption profile of atomic lines in LAS. In addition, using ultra violet diode-laser, it can measure the number density of the ground state of Fe directly without large expensive laser.

The purpose of this study is to validate this measurement technique in order to build a system for the real-time measurement of erosion rate by laser absorption spectroscopy. The anode layer type Hall thruster was used because the relation between thruster design and lifetime is not yet understood. This study aids the understanding of the trade-off between lifetime and performance.

II. Laser absorption spectroscopy

The number density of sputtered iron from thruster acceleration walls was measured, since stainless steel is generally used for the acceleration channels of anode layer type Hall thrusters. Though stainless steel consists of Fe, Cr, Ni, among other factors, the ratio of sputtered iron to eroded products is assumed to be equal to the chemical composition of it. The number density of Fe is estimated using the absorption line from ground state as shown in Fig. 1.

Number density

Number density of the ground state n_g is related to the integrated absorption coefficient K , as

$$K = \int_{-\infty}^{\infty} k_{\nu} d\nu = \frac{c^2}{\nu^2} \frac{1}{8\pi} \frac{g_e}{g_g} A_{eg} n_g \left[1 - \exp\left(-\frac{\Delta E_{ge}}{kT_{ex}}\right) \right] \quad (1)$$

Here, k_{ν} is the absorption coefficient at the frequency of ν , g is the statistical weight, the subscripts g and e denote the ground and excited states, ΔE is the energy gap and A is the Einstein coefficient. At 371.9935 nm, $g_g=9$, $g_e=11$, $\Delta E_{ge}=3.33$ eV and $A_{eg}=1.62 \times 10^7 \text{ s}^{-1}$.¹⁹

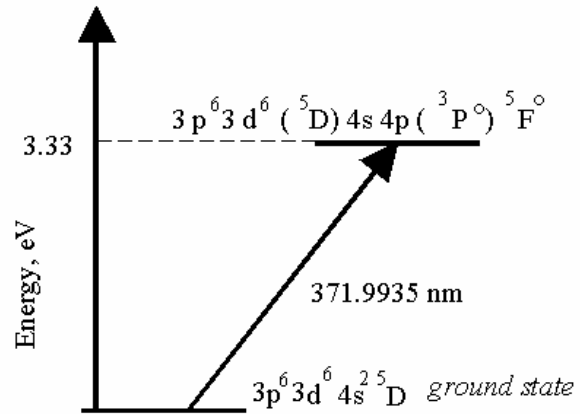


Figure1. Grotrian diagram of Fe I.

III. Experimental Equipment

A. Thruster

Figure 2 shows the cross-section of a 1 kW class anode layer type Hall thruster.²⁰ The inner and outer diameter of the acceleration channel is 48 mm and 62 mm, respectively. The outer diameter, ϕ_{out} , can be changed to 72 mm. A solenoidal coil at the center of the thruster creates a radial magnetic field in the acceleration channel. The magnetic flux density is varied by changing the coil current. The magnetic field distribution along the channel median is almost uniform in the short acceleration channel. The magnetic flux density is maximized at the inner wall and reduces with increasing radius because the magnetic flux is constant. Thus, this study assumes the magnetic flux density in the channel median to be representative. Guard rings are made of stainless steel (SUS304). For the duration erosion test, the guard rings made of copper were used instead of stainless steel in order to increase the erosion rate. The separation between the guard ring and the anode is 1 mm. The thruster has a hollow annular anode, which consists of two cylindrical rings, with a propellant gas fed through them. The width of the hollow anode is 3 mm ($\phi_{out}=62$ mm) or 8 mm ($\phi_{out}=72$ mm), and the gap between the tip of the anode and the exit of the acceleration channel is fixed at 3 mm.

High-purity (99.999% pure) xenon gas was used as the propellant. Thermal mass flow controllers (Kofloc, 3610) are used. A hollow cathode (Ion Tech HC-252) was used as the electron source.

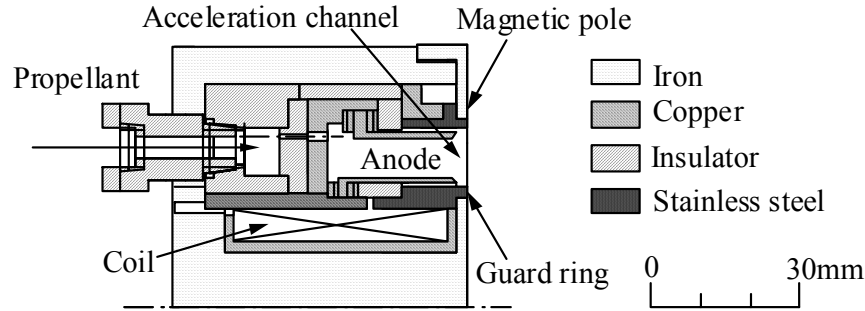


Fig.2 Cross section of the anode layer type Hall thruster developed at the University of Tokyo.

B. Vacuum Chamber

A vacuum chamber of 2 m diameter by 3 m length was used in the experiments. The pumping system consists of a diffusion pump, a mechanical booster pump and two rotary pumps. The thruster operating conditions and facility backpressure are shown in Table.1. The chamber was made of 316 stainless steel. The effect of iron eroded from the chamber wall can be neglected. Since the thruster is set at far field from the chamber wall, eroded atoms come to measurement region from the chamber wall are 1% times less than that from the thruster.

Table 1. Thruster operating conditions.

Mass flow rate		Facility backpressure
Anode	Cathode	
2.72 mg/s (± 0.05 mg/s)	0.27 mg/s (± 0.02 mg/s)	5.3×10^{-3} Pa
4.08 mg/s (± 0.05 mg/s)	0.27 mg/s (± 0.02 mg/s)	7.5×10^{-3} Pa

C. Experimental apparatus and conditions

A schematic of the measurement system is shown in Fig. 3. An ultra violet diode-laser, $Al_xIn_yGa_{(1-x-y)}N$ diode laser²¹ (Nichia, NDHU200APAE2) was used as a probe. The frequency was swept by current modulation, at a modulation width of 8 GHz. An optical chopper (Stanford Research Systems, SR540) and a lock-in amplifier (Stanford Research Systems, SR510) were used for elimination of plasma emission. The laser beam was divided in two by a beam splitter. One beam was detected by an optical spectrum analyzer (Advantest, Q8347) for the measurement of the frequency. Its resolution was 1 GHz. The other beam was used as a probe, passing in front of the thruster and being detected by a photo detector (Thorlabs, DET110/M). The laser beam was passed as shown in Fig.4 for the enhancement of sensitivity.

A monochromator (Hamamatsu Photonics, PMA-50) was used for the simultaneous measurement of the electron excitation temperature. The grating was 2,400 grooves/mm and the dispersion was 0.02 nm/ch. The wavelength resolution was 0.05 nm.

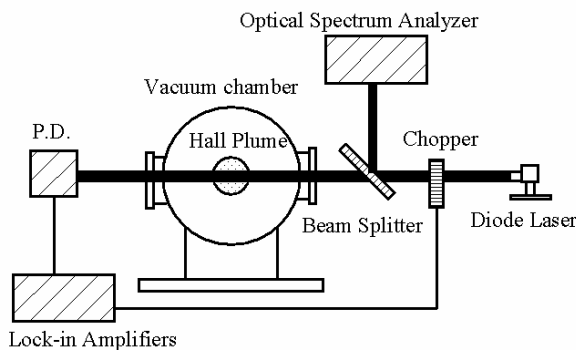


Figure3. Schematic of measurement system.

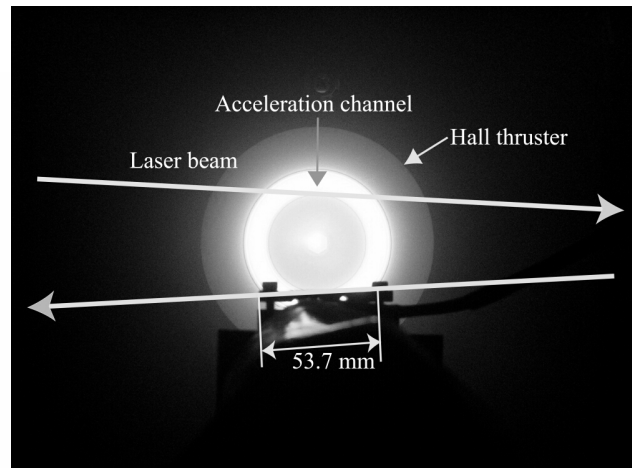


Figure 4. Appearance of Hall thruster operation.

IV. Results and Discussion

A Duration erosion test

First, duration erosion test was done in order to compare and contrast with the erosion rate by LAS. The reduction in mass of the guard rings during an hour duration test was measured. Guard rings made of copper were used instead of that made of stainless steel or carbon. Figure 5 shows the relation between the erosion rate and the magnetic flux density. The erosion rate by means of duration erosion tests decreased with magnetic flux density and beyond the critical magnetic flux density, it increased slightly, as shown in Fig. 5. At this critical magnetic flux density, the operation becomes unstable, that is, the amplitude of the discharge oscillation current at a frequency range of 10–100 kHz becomes large beyond this magnetic flux density. The erosion rate is 0.28 g/hr for operational conditions of $\phi_{out}=62$ mm, $V_d=300$ V, $\dot{m}=1.36$ mg/s and $B_r=14$ mT.

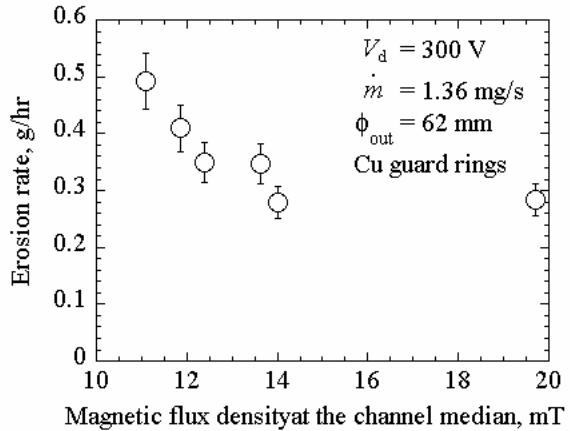


Figure 5. Relation between erosion rate and magnetic flux density by duration test.

B Laser absorption spectroscopy

There are spectra that are not used for the measurement since this laser diode has multiple longitudinal modes, as shown in Fig. 6. The line-width of the laser was less than 1GHz, which is the maximum resolution of the optical spectrum analyzer. Although lasers with multiple longitudinal modes are not adequate for laser absorption spectroscopy, there is no ultraviolet laser diode with a single longitudinal mode. In addition, there was, at the time of the experiment, no available ultra violet laser diode with an external cavity, because of the difficulty of applying anti-reflective coating. Thus, this laser was used with compensation, that is, the intensity of the absorption line was estimated by normalization of the laser intensity from the spectral distribution, since the photo detector detects the intensity of all the spectra. Figure 7 shows the ratio of the target spectrum to all spectra. It was almost constant, 0.14, during frequency modulation.

Figure 8 shows the compensated absorption profile for operational conditions of $\phi_{out}=62$ mm, $V_d=400$ V, $\dot{m}=2.72$ mg/s and $B_r=0.034$ T. Here, ϕ_{out} is the outer diameter of the acceleration channel, V_d is the discharge voltage, \dot{m} is the mass flow rate and B_r is the magnetic flux density at the channel median. The electron excitation temperature was 0.35 eV based on the Boltzmann plot for Fe I, as shown in Fig. 9. The transition data for this measurement are shown in Table 2, as quoted from the NIST database.¹⁹ Thus, stimulated emission can be neglected,

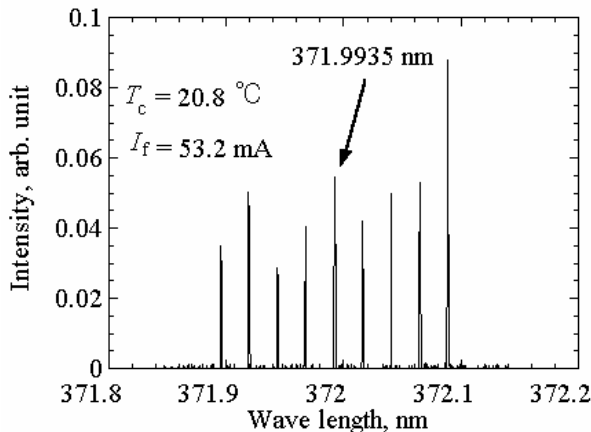


Figure 6. Spectrum of ultra violet laser diode. at $I_f=53.2$ mA.

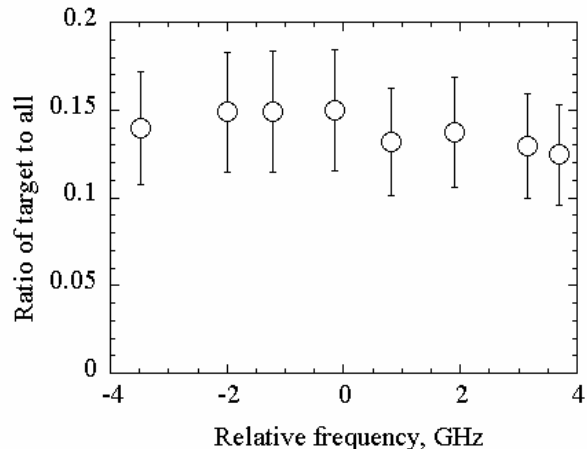


Figure 7. Ratio of target spectrum to all the spectra.

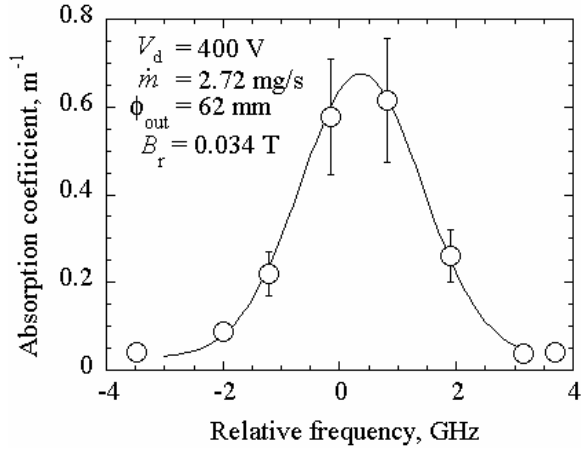


Figure 8. Absorption profile of target spectrum.

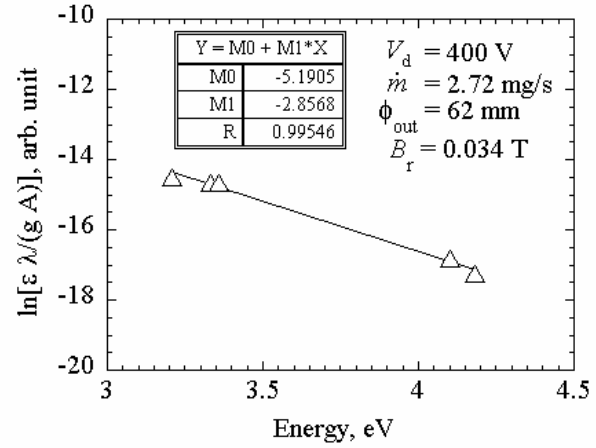


Figure 9. Boltzmann plot for Fe I.

Table 2. Transition data for Fe I.

Wave length, nm	E_k , eV	A_{ki} 10^8 s $^{-1}$	$g_i - g_k$
371.99	3.33	0.16	9 - 11
373.49	4.18	0.9	11 - 11
373.71	3.36	0.14	7 - 9
382.04	4.1	0.67	11 - 9
385.99	3.21	0.1	9 - 9

since $\Delta E_{ge}/kT_{ex} = 9.43 > 1$. The optical path length is assumed to be the crossing distance of the laser beam in front of the acceleration channel, or 0.078 m. The number density of Fe was estimated to be 1.1×10^{16} m $^{-3}$, since the number density of the ground state of Fe I would be almost equal to the that of Fe as a results of the low electron excitation temperature.

The erosion rate for these conditions was estimated to be about 0.06 g/hr from the experimental results of the wear lifetime test of this thruster. If we compensate for differences in operating conditions, discharge voltage and the sputter yield of copper and stainless steel, we arrive at 0.28 g/hr. Considering that SUS304 consists of 74% Fe, and half of the sputtered iron is assumed to leave from the thruster, the sputtering rate was estimated as

$$\dot{m}_{SUS} = 2 \times \frac{1}{0.74} SM_{Fe} N_{Fe} V_{Fe} = 0.06 \text{ g/hr} \quad (2)$$

This erosion rate is equal to 0.06 g/hr, thus, the average velocity of the Fe atoms, V_{Fe} was estimated as,

$$V_{Fe} = \frac{\dot{m}_{SUS}}{SM_{Fe} N_{Fe}} \times \frac{0.74}{2} = 2.6 \times 10^3 \text{ m/s} \quad (3)$$

This value is reasonable, since the sputtered atoms can be assumed to have about 1% of the energy of a sputtering ion,²³ or.

$$V_{Fe} = \sqrt{\frac{2eE_{Xe} \times 0.01}{M_{Fe}}} \approx 3.5 \times 10^3 \text{ m/s} \quad (4)$$

Next, the dependence of the erosion rate on operational conditions was investigated. Unfortunately, the measurement absorption rate is too small to discriminate among various conditions. Thus, the probe beam was not detected by the photo detector but by the optical spectrum analyzer. This can detect only the intensity of the target spectra, and its resolution is less than that of the photo detector.

The outer diameter of the thruster was changed to 72 mm for the enhancement of sensitivity. That is, in order to increase the absorption rate, the optical path length was increased from 0.078 m to 0.107 m. Figure 10 shows the relation between the estimated erosion rate of the guard rings and the magnetic flux density. The average velocity of

sputtered iron was estimated as in Eq. (4). The erosion rate decreased with magnetic flux density, though beyond the critical magnetic flux density, it increased slightly with magnetic flux density. This result agreed with that of duration erosion test. That is, the erosion rate by means of duration erosion tests also decreased with magnetic flux density and beyond the critical magnetic flux density, it increased slightly, as shown in Fig. 5.

The above results prove the possibility of a non-intrusive real-time erosion rate monitoring system for electric propulsion. Though this system is not strictly real-time erosion rate monitoring, but it will enable to understand the dependence of lifetime on operating conditions or thruster design without the need for long-duration tests.

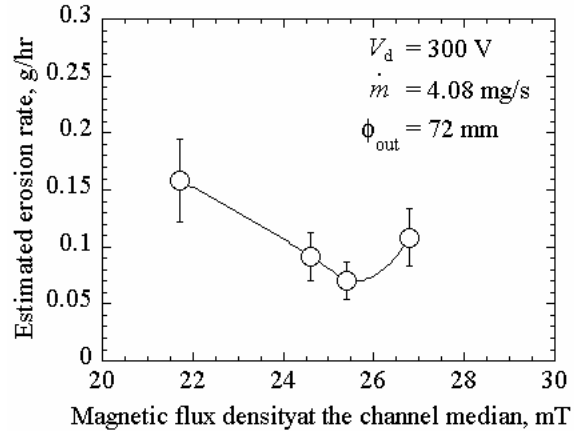


Figure 10. Relation between erosion rate and magnetic flux density.

V. Conclusion

The validity of erosion rate estimation by laser absorption spectroscopy was investigated using a 1 kW class anode layer type Hall thruster. First, the reduction in mass of the guard rings was measured in order to measure the erosion rate. The erosion rate by the duration test decreased with magnetic flux density and beyond the critical magnetic flux density, it increased slightly. The erosion rate is 0.28g/hr for operational conditions of $\phi_{out}=62$ mm, $V_d=300$ V, $\dot{m}=1.36$ mg/s, $B_r=14$ mT, and Cu guard rings. Next, the estimation of erosion rate by LAS was done. To estimate the flux of the sputtered wall material by LAS, the number density of the sputtered iron was measured using an absorption line from ground atomic iron at 371.9935 nm. An ultraviolet diode laser was used as the probe. The estimated number density of iron is $1.1 \times 10^{16} \text{ m}^{-3}$, which value is reasonable when compared with that measured by duration erosion tests. The estimated erosion rate by LAS also decrease with magnetic flux density, and beyond the critical magnetic flux density, it increase slightly with magnetic flux density. The above results prove the possibility of a non-intrusive real-time erosion rate monitoring system for electric propulsion. Though this system is not strictly real-time erosion rate monitoring, but it will enable to understand the dependence of lifetime on operating conditions or thruster design without the need for long-duration tests.

Acknowledgments

The present work was supported by a Grant-in-Aid for Scientific Research (S), No. 16106012, sponsored by the Ministry of Education, Culture, Sports, Science and Technology, Japan.

References

- 1) Saccoccia, G., "Introduction to the European Activities in Electric Propulsion," *Proceedings of the 28th International Electric Propulsion Conference*, IEPC Paper 03-341, March 2003.
- 2) Blandino, J., "The year in review, Electric propulsion" *Aerospace America*, December 2003, pp. 60-61.
- 3) Kim, V., "Main physical features and processes determining the performance of stationary plasma thrusters," *Journal of Propulsion and Power*, Vol. 14, No. 5, 1998, pp. 736-743.
- 4) Kaufman, H. R., "Technology of Closed-Drift Thrusters," *AIAA Journal*, Vol. 23, No. 1, 1985, pp. 78-86.
- 5) Choueiri, E. Y., "Fundamental difference between the two Hall Thruster Variants," *Physics of Plasmas*, Vol. 8, No. 11, 2001, pp. 5025-5033.
- 6) Zharinov, A. V., and Popov, Yu. S., "Acceleration of Plasma by a Closed Hall Current," *Soviet Physics-Technical Physics*, Vol. 12, 1967, pp. 208-211.
- 7) Garner C. E., Brophy J. R., Polk J. E., Semenkin A. V., Garlusha V. I., Tverdokhlebov S. O., Marrese C., Experimental Evaluation of Russian Anode Layer Thrusters, AIAA Paper 94-3010, 1994.
- 8) Popov, Yu. S., and Zolotaikin, Yu M., "Effect of Anomalous Conductivity on the Structure of the Anode Sheath in a Hall Current Ion Source," *Soviet Journal of Plasma Physics*, Vol. 3, No.2, March-April 1977, pp. 210-213.

- 9) Zhurin, V. V., Kaufman, H. R., and Robinson, R. S., "Physics of Closed Drift Thrusters," *Plasma Sources Science & Technology*, 8, 1999, R1–R20.
- 10) Semenkin, A., "Investigation of Erosion in Anode Layer Thrusters and Elaboration High Life Design Scheme," IEPC Paper 93-231, Sept. 1993.
- 11) Solodukhin A. E. and Semenkin, A. V.,," IEPC Paper 2003-0204, March 2003.
- 12) Garner, C.E., Brophy, J.R., Polk J.E. and Pless, L.C., " A 5,730-hr cyclic endurance test of the SPT-100," AIAA Paper 95-2667,1995.
- 13) Semenkin, A. V., Kochergin, A., Rusakov, A., Bulaev, V., Yuen, J., Shoji, J., Garner C., and Manzella, D., "Development program and preliminary test results of the TAL-110 thruster," AIAA Paper 99-2279, 1999.
- 14) Jacobson, D.T., "High Voltage TAL Erosion Characterization," AIAA Paper 02-4257, 2002.
- 15) Arroyo, M. P., Langlogis, S. and Hanson, R. K.: Diode-laser absorption technique for simultaneous measurement of multiple gasdynamic parameters in high-speed flows containing water vapor, *Applied Optics*, Vol. 33, 1994, pp.3296-3370.
- 16) Zhang, F. Y., Komurasaki, K., Iida, T., and Fujiwara, T.: Diagnostics of an argon arcjet plume with a diode laser, *Applied Optics*, Vol. 38, 1999, pp1814-1822.
- 17) Williams, G. J., Smith, T. B., Gulczinski, F. S., Gallimore, A. D., "Correlating Laser Induced Fluorescence and Molecular Beam Mass Spectrometry Ion Energy Distributions," *Journal of Propulsion and Power*, Vol. 18, No. 2, 2002, pp. 489-491.
- 18) Cedolin, R.J., Hargus, Jr., W. A., Storm, P. V., Hanson, R. K., Cappelli, M. A., "Laser-induced fluorescence study of a xenon Hall Thruster," *Applied Physics B*, 65, 1997, pp.459-469.
- 19) http://www.physics.nist.gov/PhysRefData/ASD/lines_form.html
- 20) Yamamoto N., Nakagawa, T., Komurasaki K., and Arakawa Y., "Operating Characteristics of an Anode Layer Type Hall Thruster," *Journal of the Japan Society for Aeronautical and Space Sciences*, 51, 2003, pp.492-497, (in Japanese).
- 21) S Nagahama, S., Yanamoto, T., Sano, M. and Mukai T. "Study of GaN-based Laser Diodes in Near Ultraviolet Region", *Japanese Journal of Applied Physics*, 2002, pp. 5-10
- 22) Yamamoto N., Komurasaki K., and Arakawa Y., "Control of Discharge Current Oscillation in Hall Thrusters," Proceedings of the 23rd International Symposium on Space Technology and Science, edited by J. Onodera, Japan Society for Aeronautical and Space Sciences and Organizing Committee of the 23rd ISTS, Tokyo, Japan, 2002, pp. 319 -324.
- 23) B. N. Chapman, *Glow Discharge Processes: Sputtering and Plasma Etching*, John Wiley & Sons, 1980.